Prediction of gas leakage and dispersion in utility tunnels based on CFD-EnKF coupling model

A 3D full-scale application

Cai, Jitao; Wu, Jiansong; Yuan, Shuaiqi; Kong, Desheng; Zhang, Xiaole

DOI
10.1016/j.scs.2022.103789

Publication date
2022

Document Version
Final published version

Published in
Sustainable Cities and Society

Sustainable Cities and Society 80 (2022) 103789

Contents lists available at ScienceDirect

Sustainable Cities and Society

journal homepage: www.elsevier.com/locate/scs

Prediction of gas leakage and dispersion in utility tunnels based on CFD-EnKF coupling model: A 3D full-scale application

Jitao Cai [a], Jiansong Wu [a,*], Shuaiqi Yuan [b], Desheng Kong [a], Xiaole Zhang [c]

[a] School of Emergency Management & Safety Engineering, China University of Mining and Technology, Beijing 100083, China
[b] Safety and Security Science Section, Faculty of Technology, Policy and Management, TU Delft, Delft, the Netherland
[c] Institute of Environmental Engineering, ETH Zürich, Zürich, CH-8093, Switzerland

ARTICLE INFO

Keywords:
Utility tunnel
Gas leakage
Computational fluid dynamics
Ensemble Kalman filter
OpenFOAM

ABSTRACT

Natural gas compartment accommodated in utility tunnels is beneficial in meeting the pressing demand of energy supply and sustainable urban environment. However, the leaking gas characterized by flammable and explosive can pose a huge threat to the safe operation of the utility tunnel. When an unexpected gas leakage accident happens in the actual situation, the prior information associated with the leakage source is commonly unclear or unknown. Therefore, the absence of an available tool for reasonable leakage and dispersion prediction in the above scenario precludes the timely and appropriate emergency response treatment. In this study, a three-dimensional source term estimation (3D-STE) model with the combination of the computational fluid dynamics (CFD) and ensemble Kalman filter (EnKF) algorithm is proposed to achieve spatiotemporal gas concentration prediction and gas emission source estimation. In the proposed approach, the observation data can be incorporated into the gas dispersion simulations continuously, thus the simulation results can be revised by the observation data and the source term estimation of gas leakage can be achieved by employing the EnKF algorithm. A twin experiment is employed to validate the effectiveness and practicability of the proposed model. The results show that the proposed model can revise the prior errors in the gas leakage rate significantly and obtain an accurate prediction of gas concentration distribution as well as gas leakage rate. A feasible framework is also proposed serving as a good paradigm for the 3D-STE model application. This study helps for consequence assessment and emergency response of gas leakage accidents in utility tunnels.

1. Introduction

With the worldwide trend of rapid urbanization, there are increased demands for sustainable cities development (Broere, 2016; Marzouk & Othman, 2020). The construction of utility tunnels leads to an upsurge of interest because it shows a great advantage in the clean energy supply and urban planning (Wang, Tan, Xie & Ma, 2018; Yang, Peng, Xu & Zheng, 2019; Yin, Liu, Chen, Wang & AI-Hussein, 2020). However, many types of municipal pipelines (e.g., gas pipelines, sewage pipelines, heating pipelines, and water supply pipelines) are housed in utility tunnels, which causes a spatial concentration of multiple hazards (Bai, Zhou & Wu, 2020). As one of the most threatening hazards in utility tunnels, natural gas pipelines have attracted a most widespread concern because the leakage of gas may cause fire, explosion, and other cascading accidents. Meanwhile, the leakage of natural gas is also an environmental concern since methane is an extremely environment-harmful greenhouse gas that can speed up global warming (Cai, Wu, Yuan, Liu & Kong, 2021). Therefore, gas leakage in utility tunnels can cause unexpected and severe consequences in the context of casualties, economic losses, and environmental problems, which should be given sufficient attention from the perspective of consequence assessment and emergency response.

Natural gas pipeline leakage in utility tunnel scenarios was mainly investigated by previous studies through CFD simulations as well as some reduced-scale experiments (Wang, Tan, Zhang, Zhang & Yu, 2020). first employed a two-dimensional numerical model to investigate the effect of leakage size, pipeline pressure, and mechanical ventilation on gas dispersion in utility tunnels. However, the complex environment in utility tunnels caused by mechanical ventilation and the obstruction from facilities brings huge difficulties to gas dispersion simulation. Such tricky situations may not be well resolved by a simplified two-dimensional model (Li, Liu, Wang, Zheng & Deng, 2019; Lu, Huang,

* Corresponding author.
E-mail address: jiansongwu@hotmail.com (J. Wu).

https://doi.org/10.1016/j.scs.2022.103789
Received 2 December 2021; Received in revised form 24 January 2022; Accepted 16 February 2022
Available online 18 February 2022

Fu, Zhang, Wu & Lyu, 2018). Therefore, the three-dimensional numerical model for simulating the gas leakage accidents in utility tunnel scenarios has attracted more and more attention in recent years (Li, Liu, Wang, Zheng & Deng, 2019; Lu, Huang, Fu, Zhang, Wu & Lyu, 2018; Tan, Liu & Wang, 2017; Zhang & Lan, 2020; Bu, Liu, Wang, Xu, Chen & Hao, 2021; Zhou, Li, Cai, Yang, Peng & Chen 2021). Tan, Liu & Wang (2017) compared dispersion characteristics of two kinds of gravity gases considering whether there is an available ventilation mode. The results indicated that ventilation can disrupt the concentration stratification and reduce gas accumulation. Liu, Wang, Guo, Zhang & He (2019) employed the realizable k-epsilon model to study the gas diffusion taking into account ambient temperature and humidity. It revealed that the kinetic energy of methane molecular motion was proportional to temperature, which subsequently caused a larger diffusion coefficient and more rapid spread of natural gas. Zhang & Lan (2020) investigated the effect of ventilation velocities and sizes on the gas dispersion behaviors in the utility tunnels. Meanwhile, the optimal ventilation configurations were proposed from the aspect of economy, efficiency, and safety. Zhou, Li, Cai, Yang, Peng & Chen (2021) and Zhou, Li, Cai, Jiang, Zhuang & Li, (2022) built a utility tunnel mockup and the accuracy of the random opening air supply model and standard k-epsilon turbulence model was confirmed through numerical and experimental comparison. Moreover, gas monitoring sensor networks are optimized through the CFD-adjoint-based method. Bu, Liu, Wang, Xu, Chen & Hao (2021) conducted a multi-factor analysis to study the gas dispersion characteristics in utility tunnels. The methane invasion distance (MID) equation was also concluded, which helps to provide a reference for the installation of gas alarm devices. Except for investigating the gas dispersion process influenced by multiple factors, Lu, Huang, Fu, Zhang, Wu & Lyu (2018) presented a numerical analysis with an emphasis on rush repairs, such as optimizing the configurations of block valves and ventilation fans. As shown in the above studies, the CFD simulations have great advantages in evaluating the consequence of specific gas leakage scenarios without initial parameters uncertainty. However, there are still varying degrees of errors in the prediction of gas leakage and dispersion by using CFD techniques when an unexpected leakage accident occurs in the actual situation. These errors primarily stem from the lack of source term information and wind field perturbation induced by mechanical ventilation and complex facility layouts. Such an ill-posed problem can deviate the simulation results from actual situations significantly, which prohibits real-time consequence assessment and reasonable emergency response treatment.

Source term estimation (STE) methods are developed to identify the unknown source information based on limited and noisy observation data, which has great potential in leakage source estimation and error suppression. As the two most attractive and dominant approaches of STE methods (Wu, Liu, Yuan, Cai & Hu, 2020; Xue, Kikumoto, Li & Ooka, 2018), many optimization-based and probabilistic-based methods have been used to accomplish the inverse problem of gas dispersion, such as the ensemble Kalman filter method (Wang, Zhao, Lei & Wang, 2019; Wu, Cai, Yuan, Zhang & Reniers, 2021; Zhang & Huang, 2017; Zhang, Su, Chen, Raskob, Yuan & Huang, 2015b; Zhang, Li, Su & Yuan, 2015a) and Bayesian inference method (Wang, Huang, Huang & Ristic, 2017; Xue, Kikumoto, Li & Ooka, 2018; Xue, Li & Zhang, 2017). Moreover, data-driven methods were also adopted to achieve source term estimation with the rapid development of machine learning and deep learning (Kim, Park, Kim & Shin, 2019; Ma & Zhang, 2016; Ma, Gao, Zhang & Zhao, 2021). However, the current associated with source term estimation are mainly restricted to atmospheric environment scenarios. Utility tunnels characterized by confined and ventilated space poses great difficulties for source term estimation and accurate gas dispersion prediction, which needs to be further investigated. Yuan, Wu, Zhang & Liu (2019) and Wu, Liu, Yuan, Cai & Hu (2020) have proposed an EnKF-based model and Bayesian inference-based model, respectively for predicting the gas dispersion process and reconstructing the leakage source in utility tunnels. However, the gas transport process is determined on the basis of the one-dimensional advection-diffusion equation, which has significant difficulties in handling the three-dimensional facilities layout, turbulent diffusion, and gravity-driven multicomponent transportation. Therefore, the further endeavor could be the development of the high confidence three-dimensional gas dispersion model and combining it with the source term estimation method. This can help to reproduce a more realistic gas dispersion scenario as well as the estimation of the leakage source. Moreover, dynamic ventilation conditions adopted in the operation of utility tunnels in real leakage situations have not been fully considered. This may lead to some inaccuracy in the prediction of gas leakage and dispersion process, which represents a practical issue that needs to be addressed.

In this study, a three-dimensional source term estimation model is proposed to improve the prediction accuracy of gas leakage and dispersion in utility tunnels. Firstly, the three-dimensional CFD-based gas dispersion model is developed based on the OpenFOAM platform and validated by experimental data. Then, the 3D-STE model can be built by combining the gas dispersion model and the EnKF algorithm. Furthermore, a twin experiment is employed to validate the proposed model considering the dynamic ventilation condition of utility tunnels. The effectiveness of the proposed model is evaluated qualitatively and quantitatively in the twin experiment in terms of gas concentration distribution and source term (leakage velocity) estimation. This study can provide effective technical support for safety control and emergency response of gas leakage accidents in utility tunnels.

2. Methodology

The proposed 3D-STE model consists of the CFD-based gas dispersion model and the EnKF algorithm. In this section, the basic equations related to the gas dispersion model and the EnKF algorithm are introduced, respectively. Furthermore, the specific procedure for conducting the proposed model is elaborated.

2.1. Governing equation of CFD model

In this study, a three-dimensional compressible CFD solver based on the OpenFOAM platform is developed for the simulation of gas leakage and dispersion in the utility tunnel (Mack & Spruijt, 2013; Fiates, Santos, Neto, Francesconi, Simoes & Vianna 2016; Wu, Cai, Yuan, Zhang & Reniers 2021). The OpenFOAM platform allows the integration of the EnKF algorithm and the gas dispersion simulation expediently due to its high extensibility. The governing equations adopted from OpenFOAM are presented as follows:

(i) Continuity equation

$$\frac{\partial \rho}{\partial t} + \nabla\cdot(\rho \boldsymbol{u}) = 0 \tag{1}$$

(ii) Momentum equation

$$\frac{\partial(\rho u)}{\partial t} + \nabla\cdot(\rho u \boldsymbol{u}) = -\frac{\partial p}{\partial x} + \nabla\cdot(\mu\nabla u) + F_x \tag{2}$$

$$\frac{\partial(\rho v)}{\partial t} + \nabla\cdot(\rho v \boldsymbol{u}) = -\frac{\partial p}{\partial y} + \nabla\cdot(\mu\nabla v) + F_y \tag{3}$$

$$\frac{\partial(\rho w)}{\partial t} + \nabla\cdot(\rho w \boldsymbol{u}) = -\frac{\partial p}{\partial z} + \nabla\cdot(\mu\nabla w) + F_z \tag{4}$$

(iii) Energy equation

$$\frac{\partial(\rho i)}{\partial t} + \nabla\cdot(\rho i u) = -p\nabla\cdot u + \nabla\cdot(k\nabla T) + \phi + S_h \tag{5}$$

(iv) Multi-component transport equation

$$\frac{\partial}{\partial t}(\rho C_i) + \nabla\cdot(\rho C_i \boldsymbol{u}) = \nabla\cdot(D\nabla C_i) + S_i \tag{6}$$

(v) Gas state equation

$$pV = nZRT \tag{7}$$

Where ρ is the mixed gas density, u is the gas velocity vector. p is the pressure, μ is the viscosity, F_x, F_y and F_z are the momentum source term in three directions. i and T are internal thermal energy and temperature, respectively. k is the thermal conductivity coefficient, S_h is the internal heat source, and Φ is the dissipation function. C_i represents the gas volume fraction of every species, D is diffusion capacity coefficient and S_i is mass source term. V, n, Z, R are gas volume, amount of substance, compressibility, and the gas constant, respectively.

As a robust two-equation eddy-viscosity turbulence model, the shear stress transport (SST) turbulence model was employed to simulate the turbulent flow (Sklavounos & Rigas, 2004). And the corresponding equations are listed:

$$\frac{\partial(\rho k)}{\partial t} + \nabla\cdot(\rho k\boldsymbol{u}) = \nabla\cdot((\mu + \sigma_k\mu_t)\nabla k) + P - \rho\beta^*\omega k \tag{8}$$

$$\frac{\partial(\rho\omega)}{\partial t} + \nabla(\rho\omega\boldsymbol{u}) = \nabla\cdot((\mu +_{\omega}\mu_t)\nabla\omega) + \frac{\gamma}{\nu_t}P - \rho\beta\omega^2 + 2(1 - F_1)\frac{\rho_{\omega 2}}{\omega}\nabla k\nabla\omega \tag{9}$$

Where k and ω represent turbulence kinetic energy and turbulence dissipation rate. P is the production rate of turbulence, μ_t is turbulence viscosity. The SST turbulence model combines the k-epsilon and k-omega model through a blending factor F_1. The k-omega model is utilized in the region close to the boundary layer and switches to the k-epsilon model in the vicinity of the free shear flow. The detailed description and specific values of model parameters are summarized in Menter's study (Menter, Kuntz & Langtry, 2003).

2.2. Ensemble Kalman filter algorithm

Due to the implicit assumption of linear Gaussian state-space, the Ensemble Kalman filter algorithm has a great advantage in avoiding the degeneracy problem of reweighting-based data assimilation algorithms (Katzfuss, Stroud & Wikle, 2016). It promotes the wide application of the EnKF algorithm in various scenarios because of its remarkable robustness, such as river pollution scenarios (Wang, Zhao, Lei & Wang, 2019; Zhang & Huang, 2017), nuclear disasters scenarios (Zhang, Li, Su & Yuan, 2015a, Zhang, Su, Chen, Raskob, Yuan & Huang, 2015b), indoor pollution scenario (Lin & Wang, 2013; Sharma, Vaidya & Ganapathysubramanian, 2019), chemical plant scenario (Wu, Cai, Yuan, Zhang & Reniers, 2021), and confined space scenarios (Ji, Tong, Wang, Lin, Zhang & Gao, 2018; Wu, Yuan, Zhang & Zhang, 2018; Yuan, Wu, Zhang & Liu, 2019).

In this section, the basic equations of the EnKF algorithm are presented as follows:

(i) Forcast step:

$$X_t^f = M\left(X_{t-1}^f\right),\ X_t^f \in R^{n*N} \tag{10}$$

(ii) Analysis step:

$$X_t^a = X_{t-1}^f + K\left(Y_t^* - H * X_t^f\right) \tag{11}$$

Where Eqs. (10) and (11) represent the main procedure of the EnKF algorithm, X_t^f is the state matrix at time t, it usually has n rows and N columns, n and N represent the parameters of interest and ensemble sizes, respectively, X_t^a is analytical value revised by observation data. The M stands for the nonlinear dynamic model propagating state matrix over time, and H is a nonlinear observation operator transforming the state matrix to the corresponding observation sites. K represents the Kalman gain.

The forecast error covariance matrix can be calculated by Eq. (12).

$$P = \frac{1}{N-1}\left(X_t^f - \overline{X_t^f}\right)\left(X_t^f - \overline{X_t^f}\right)^T \tag{12}$$

Where P is the forecast error covariance matrix, $\overline{X_t^f}$ can be obtained by multiplying an average factor 1_N with N rows and N columns and every factor in 1_N is $1/N$.

The Kalman gain K serves as a weighted factor between the gas dispersion CFD model prediction and observation data. It can be obtained by Eq. (13).

$$K = PH^T\left(HPH^T + R_e\right)^{-1} \tag{13}$$

Where R_e is the observation error covariance matrix and can be calculated as follows:

$$E^{obs} = (\varepsilon_1,\ \varepsilon_2, \varepsilon_3, \varepsilon_4 \ldots \varepsilon_k) \tag{14}$$

$$R_e = E^{obs} * \left(E^{obs}\right)^T \tag{15}$$

Where E^{obs} is the observation error vector and ε represents the perturbation added to observation data.

In this study, the state matrix consists of N ensembles, and every vector contains gas concentrations and leakage velocity:

$$X = (x_1, x_2, x_3 \ldots x_N) \in R^{n*N} \tag{16}$$

$$x_N = (c_1, c_2, c_3 \ldots c_m\ , u_1 \ldots u_l,)^T \in R^{n=i+l} \tag{17}$$

Where x is the state vector, c is the leaked gas concentration. and u means the leakage velocity at the leakage hole. Moreover, m represents the total grid number including concentration data, l is the number of data assimilation steps. u_1 represent the initial-guess leakage velocity, which should be prescribed by users. Then, a new leakage velocity will be updated and added in the state vector x once a data assimilation step is completed.

$$u_l^b = \sum_{i=1}^{N} u_{l-1}^a(i) \Big/ N \tag{18}$$

$$u_l^f(i) = u_l^b + \delta\ u_l^b(i) \tag{19}$$

Where $u_{l-1}^a(i)$ is the revised leakage velocity of the latest time step at corresponding ensemble i, the ensemble average leakage velocity u_l^b is used to generate the new leakage velocity ensemble for the next time step by adding noise $\delta\ u_l^b(i)$, which can be calculated by Eq. (20).

$$\delta\ u_l^b(i) = \alpha u_{l-1}^a(i) + \sqrt{1-\alpha^2}\ r_{l-1}(i)\sigma \tag{20}$$

Where α represents the influence of the latest leakage velocity on the determination of the leakage velocity at the next time steps and is set as 0.99 in this study. $r_{l-1}(i)$ is a random number following Gaussian distribution $N \sim (0,1)$. And σ is the standard deviation of the latest leakage velocity ensemble u_{l-1}^a.

2.3. Three-dimensional STE model

With the combination of the CFD-based gas dispersion model and EnKF algorithm, the three-dimension STE model can be developed. The EnKF algorithm allows integrating the observation data into the three-dimensional gas dispersion model and helps to suppress errors resulting from the numerical simulation and the observation sensors/sites. It helps to improve the prediction accuracy of the spatial-temporal distribution of leaked gas and further achieves a reasonable leakage source estimation in utility tunnels. The complex scenarios in utility tunnels are characterized by the confined underground space equipped with various facilities and forced ventilation. Such complex scenarios bring huge difficulties to the inversion models. The inverse problems in utility tunnels have not been resolved well by previous studies in the aspect of both source term estimation and three-dimensional gas concentration prediction. The specific implementation of the three-dimensional STE model is presented in Fig. 1.

Generally, the leakage source term is unknown when an unexpected leakage accident happened in real situations. The leakage source distribution with inevitable prior errors should be initialed by users in the CFD model to conduct gas leakage and dispersion simulations. The prior leakage source term and corresponding gas concentration distribution results will be revised by the EnKF algorithm whenever the observation data is available. Finally, the revised leakage source and gas concentration distribution are utilized to reconstruct the revised state matrix for the next iteration. As the data assimilation process goes on, the revised predictions of gas concentration distribution and gas leakage source term can be obtained.

3. Model validations

3.1. Validation of gas dispersion model

Generally, the unsatisfactory performance of the gas dispersion model will greatly weaken the accuracy of the estimation method (Ma & Zhang, 2016; Ma, Gao, Zhang & Zhao, 2021). In order to illustrate the gas dispersion model can capture the detailed flow field when an accidental leakage occurs. It is common practice that the experimental data are used to be compared with the prediction results of the gas dispersion model. Most existing experiments, also numerical model validation, associated with gas leakage in the utility tunnel use alternative gases such as CO_2 and neon due to the potential fire/explosion risk by using methane (Bu, Liu, Wang, Xu, Chen & Hao, 2021; Zhou, Li, Cai, Yang, Peng & Chen, 2021; Wang, Tan, Zhang, Zhang & Yu, 2020). Considering both the feasibility for model validation and the availability of the experiment data, the experimental data obtained from (Fang, Lin, Huang and Zheng, 2006) are employed to validate the feasibility and accuracy of the gas dispersion model.

3.1.1. Numerical configurations

In Fang's study, a reduced-scale utility tunnel system was designed to investigate the gas dispersion process in the confined space, and the quantitative comparison by using numerical simulation was also involved. The investigated utility tunnel has a dimension of 10 $m \times 0.15$ $m \times 0.15$ m, which is displayed in Fig. 2. A rectangular window with a dimension of 0.01 $m \times 0.01$ m was set as the gas vent. Carbon dioxide was utilized as an alternative gas to methane considering safety requirements. The CO_2 gas was released from a circular hole with a diameter of 0.02 m. Meanwhile, a total of 49 gas sensors were employed to detect the CO_2 concentration along the centerline of the utility tunnel mode. The distance between two gas sensors is set as 0.2 m. The specific parameters related to this experiment are listed in Table 1.

As shown in Fig. 2, the computational domain of the utility tunnel model is discretized by using a hexahedral cell scheme (Duan, Liu, Xu, Huang, Shen & Lin, 2015). To avoid the sharp aspect ratio of cells, the computational domain is divided into two sub-parts for hexahedral discretization. Such operation will cause a misaligned mesh interface but can be handled by the arbitrary mesh interface (AMI) technique (Carneiro, Moura, Rocha, Lima & Ismail, 2019).

By referring to the experimental configuration in Fang's study, the specific boundary conditions applied in this study are summarized as follows:

(i) Inlet: *flowRateInletVelocity* condition is employed to provide a stable volumetric flow rate, which is set as 4 L/min.
(ii) Outlet: *pressureInletOutletVelocity* condition is used to serve as a pressure outlet, and the pressure value is prescribed as 101,325 Pa.
(iii) Mesh interface: *cyclicAMI* condition is introduced to handle the data exchange by interpolation calculation.
(iv) Walls: All the walls are defined as the *no-slip* condition.

3.1.2. Results analysis

Firstly, mesh independence analysis was conducted to ensure the mesh-independent results. The CO_2 concentration along the sampling centerline (mentioned in Table 1) at 120 s was utilized to evaluate the

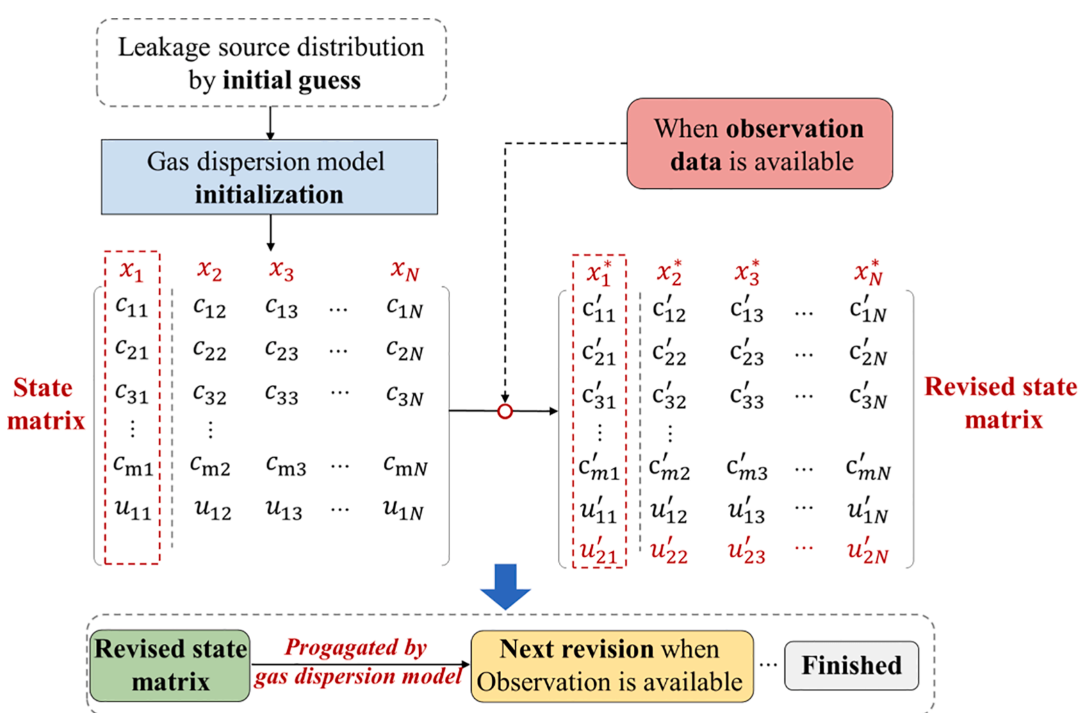

Fig. 1. Specific implementation of three-dimensional STE model.

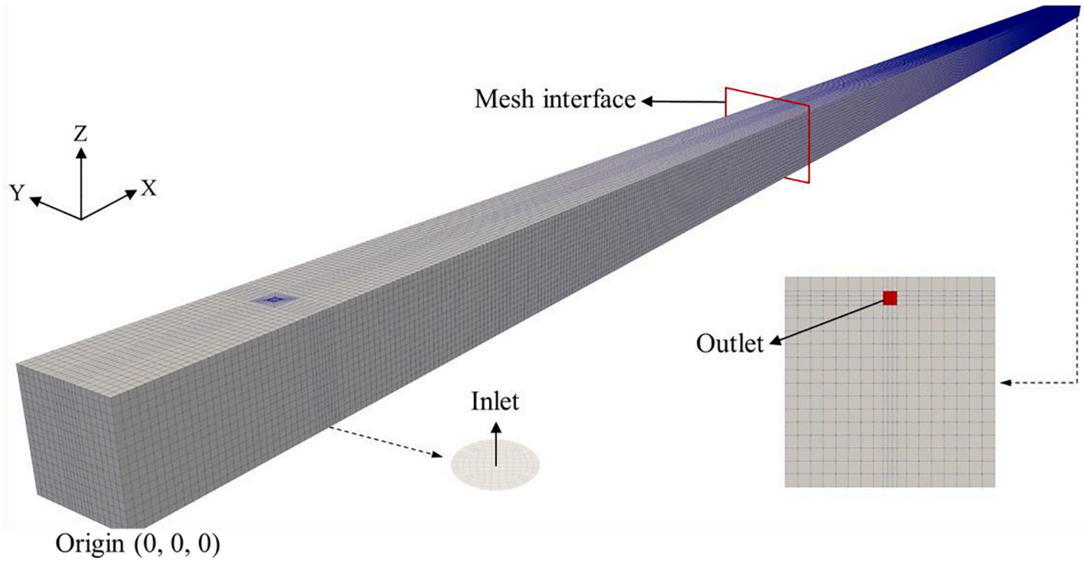

Fig. 2. Geometric and mesh schematic of the utility tunnel system.

Table 1
Specific configurations of the gas release experiment.

Parameter	Value
Length of the utility tunnel system (m)	10
Width of the utility tunnel system (m)	0.15
Height of the utility tunnel system (m)	0.15
Location of leakage hole (m)	(0.28, 0, 0)
Location of the sampling centerline (m)	(0, 0.075, 0.075) to (10, 0.075, 0.075)
Location of NO.16 gas sensor (m)	(3.1, 0.075, 0.075)
Release flow rate (L/min)	4
Environmental temperature (K)	293
Total experiment time (s)	300

differences between four mesh schemes. The comparison of the simulation results obtained by using four different mesh schemes with grid numbers of 100 thousand, 200 thousand, 300 thousand, and 400 thousand is presented in Fig. 3. As shown in Fig. 3, although the simulation results of four mesh schemes have a similar tendency, Mesh_1 and Mesh_2 schemes have a relatively large deviation in both CO_2 concentration and dispersion distance compared to the Mesh_3 scheme. As the stepwise refinement of grids, there is a reasonable difference between Mesh_3 and Mesh_4 schemes (the max relative error and average relative error are 8.79% and 1.55%, respectively). Therefore, Mesh_3 is considered suitable for the following simulations and analysis with both acceptable accuracy and low computational load.

In order to validate the gas dispersion model quantitatively, CO_2 monitoring data obtained from (Fang, Lin, Huang & Zheng, 2006) were adopted for further comparison Fig. 4. presents the CO_2 concentration comparison between simulation results and experimental data at the location of the No.16 gas sensor (mentioned in Table 1). As shown in Fig. 4, There is one relatively large deviation between simulation results and experimental data at 60 s with a 34% relative error, which can be seen in Fang'study similarly. The reason for this may be the uncontrollable error induced by measurement equipment and the ambient environment. Overall, the simulation results of the gas dispersion model achieved a reasonable agreement with the experimental data. Most of the relative errors between the simulation results and experimental data are less than 10.00%. And the average relative error between simulations and experimental data is 9.73%. It indicates that the gas dispersion model can well capture the dispersion behaviors of gravity-driven gas flow in the confined space scenario (Wang, Tan, Zhang, Zhang & Yu, 2020; Zhang & Lan, 2020). Therefore, it can be used for the prediction of

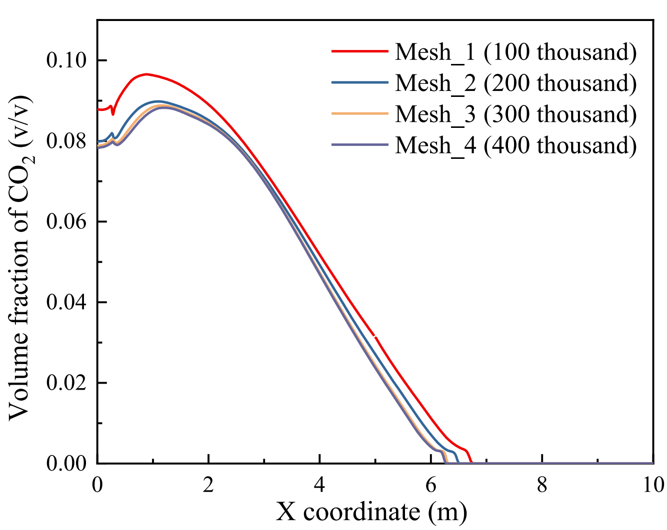

Fig. 3. Mesh independence analysis.

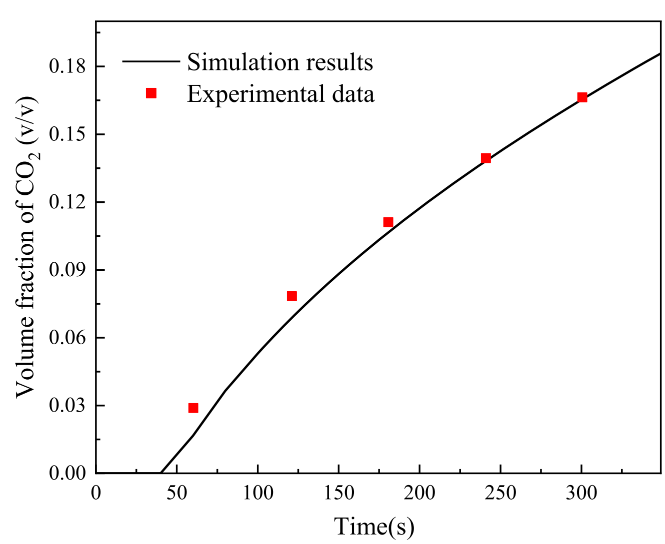

Fig. 4. CO_2 concentration comparison at the No.16 gas sensor.

gas leakage and dispersion in utility tunnel scenarios with good accuracy.

3.2. 3D-STE model validation

After the validation of the gas dispersion model, it can be integrated with the EnKF algorithm to achieve the gas dispersion prediction and leakage source estimation in the utility tunnel. A twin experiment, which was already been applied for evaluating the data assimilation models (Yuan, Wu, Zhang & Liu, 2019; Zhang, Su, Yuan, Chen and Huang, 2014), was employed to validate the effectiveness and practicability of the proposed 3D-STE model.

3.2.1. Configurations

In this section, the computational domain is built and discretized by using the blockMesh and snappyHexMesh tools, which are involved in the OpenFOAM platform for the hexahedral mesh generation. The configuration of the computational domain was determined by referring to the underground utility tunnel of Changbin Road in Haikou City. The geometric layout and boundary conditions of the computational domain are shown in Fig. 5. Moreover, Table 2 summarizes the configuration parameters related to the calculations.

The determination of the adopted boundary conditions and the corresponding parameter values is presented as follows:

(1) Inlet: The user-defined *codedFixedValue* condition is used to provide a time-dependent ventilation condition considering the dynamic transformation of air exchange frequency when an unexpected leakage accident occurs in the utility tunnel. By referring to Eq. (21) (Ministry of Housing and Urban-Rural Development of the People's Republic of China, 2015), the ventilation velocities of the Inlet are set as 1.6 m/s and 3.2 m/s for normal ventilation and accidental ventilation scenarios, respectively.

$$v_{Inlet} = \frac{n \times V}{3600 \times F} \tag{21}$$

Where n is the air exchange frequency, F is the area of the ventilation vent, and V represents the volume of the utility tunnel.

Table 2
Configuration parameters of the utility tunnel.

Parameter	Value
Length of the utility tunnel (m)	200
Width of the utility tunnel (m)	2
Height of the utility tunnel (m)	2.4
Location of leakage hole (m)	(45, 0.9, 0.6)
Diameter of leakage hole (mm)	100
Diameter of the gas pipeline (mm)	500
Normal air exchange frequency (h^{-1})	6
Accidental air exchange frequency (h^{-1})	12
Environmental temperature (K)	293

(1) Outlet: The pressureInletOutletVelocity condition is employed to define a pressure outlet, and the pressure value is set as 101,325 Pa.
(2) Leak: The fixedValue condition is selected to define a stable leakage velocity and the leakage velocity of the leakage hole is set as 15 m/s.
(3) Walls: All the walls are defined as the *noSlip* condition.

Moreover, in order to model a more real leakage scenario, the steady flow field without leakage is computed firstly to initialize the internal flow fields for the leakage scenario.

The above-mentioned configuration parameters were utilized in the control group of the twin experiment for representing an assumed real situation (using initial parameters without uncertainty). In the data assimilation (DA) group of the twin experiment, the initial-guess parameters are employed. Thus the effectiveness of the 3D-STE model can be validated by comparing the difference between the control group and the DA group. In this study, the initial-guess leakage velocity ensemble is assumed to follow a uniform distribution, which can be observed in Fig. 6. Meanwhile, a normal distribution noise of $N \sim (0,\ 0.1)$ is added to the airflow ensemble considering the uncertainty resulting from ventilation perturbation in the confined space Fig. 7. presents 84 observation sites in the control group. The corresponding collected observation data will be utilized to revise the concentration distribution and reconstruct the gas leakage rate of the DA group. And ensemble Inflation is used to modify the prior ensemble estimates of the state matrix to reduce filter error and avoid filter divergence (Anderson, 2007). Finally, the detailed configuration parameters used in the three-dimensional STE model are listed in Table 3.

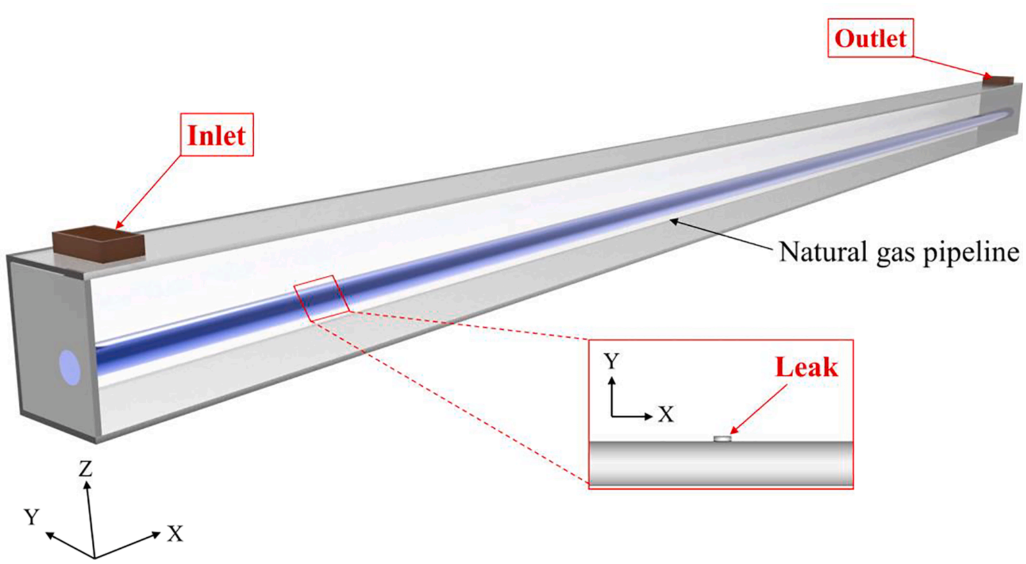

Fig. 5. Geometric and boundary conditions of the utility tunnel.

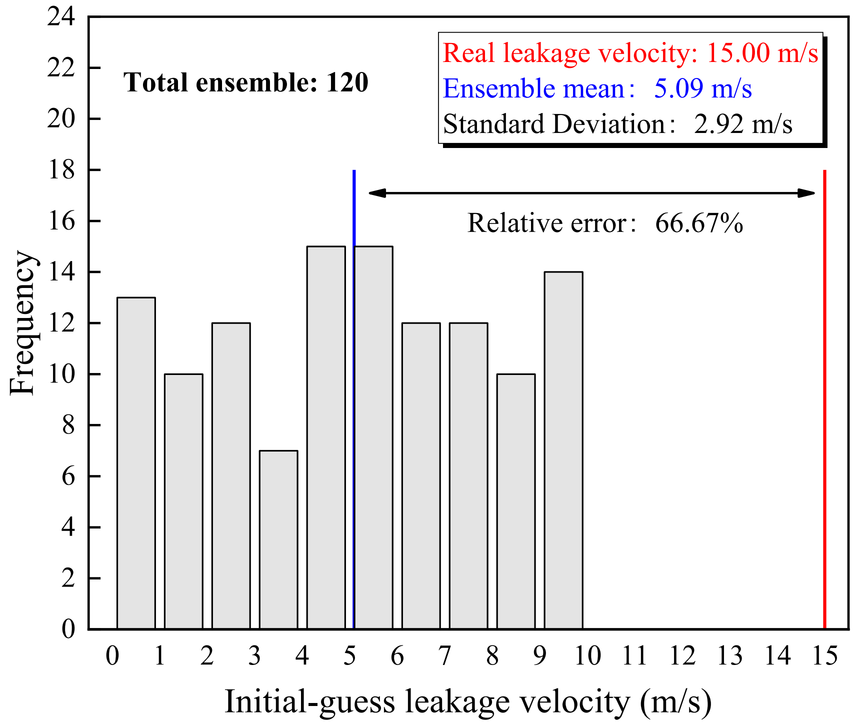

Fig. 6. Prior leakage velocity ensemble obtained by initial guess.

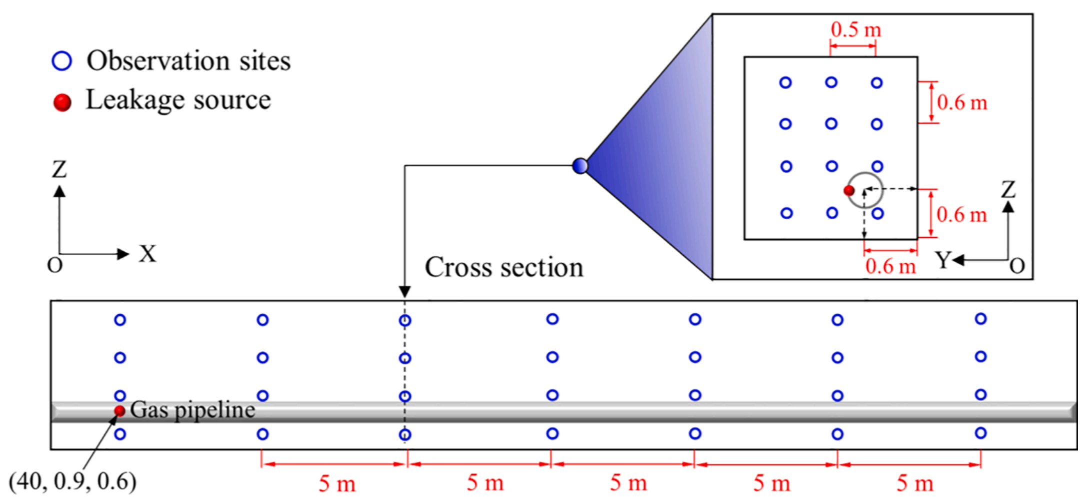

Fig. 7. Specific layout of the observation sites.

Table 3
Configuration parameters of the 3D-STE model.

Parameter	Value
Ensemble size	120
Ensemble inflation	1.0
Observation site number	84
Data assimilation frequency (s^{-1})	0.5
Total simulation time (s)	30
Total data assimilation steps	60

3.2.2. Prediction of gas spatiotemporal distribution

According to the regulation of GB50838-2015 *Technical Specification for Urban utility Tunnel Engineering*, the air exchange frequency will shift from 3 to 6 when the gas alarm threshold (1% VOL) is reached. This dynamic transformation of ventilation conditions can bring perturbation to the flow field, especially for the confined space with facilities. In this section, such dynamic and complex scenarios will be used to test the effectiveness of the proposed model with both qualitative and quantitative comparisons.

Figs. 8 and 9 present the horizontal (X = 40 m cross-section) and vertical (Y = 1 m cross-section) comparisons of gas concentration distributions obtained from the control group, DA group, and reference group. The reference group was present here for demonstrating prediction results without the DA revision (i.e., activating the gas dispersion model only by initial-guess leakage velocity and no observation data is integrated). The leakage velocity of the reference group is set as the mean of the initial-guess ensemble (5.09 m/s). Thus, the effectiveness of the proposed model can be observed directly by comparing the difference between the control group, DA group, and reference group. As can be seen from Fig. 8, the gas concentration distribution between the DA group and the reference group has no apparent difference at the initial

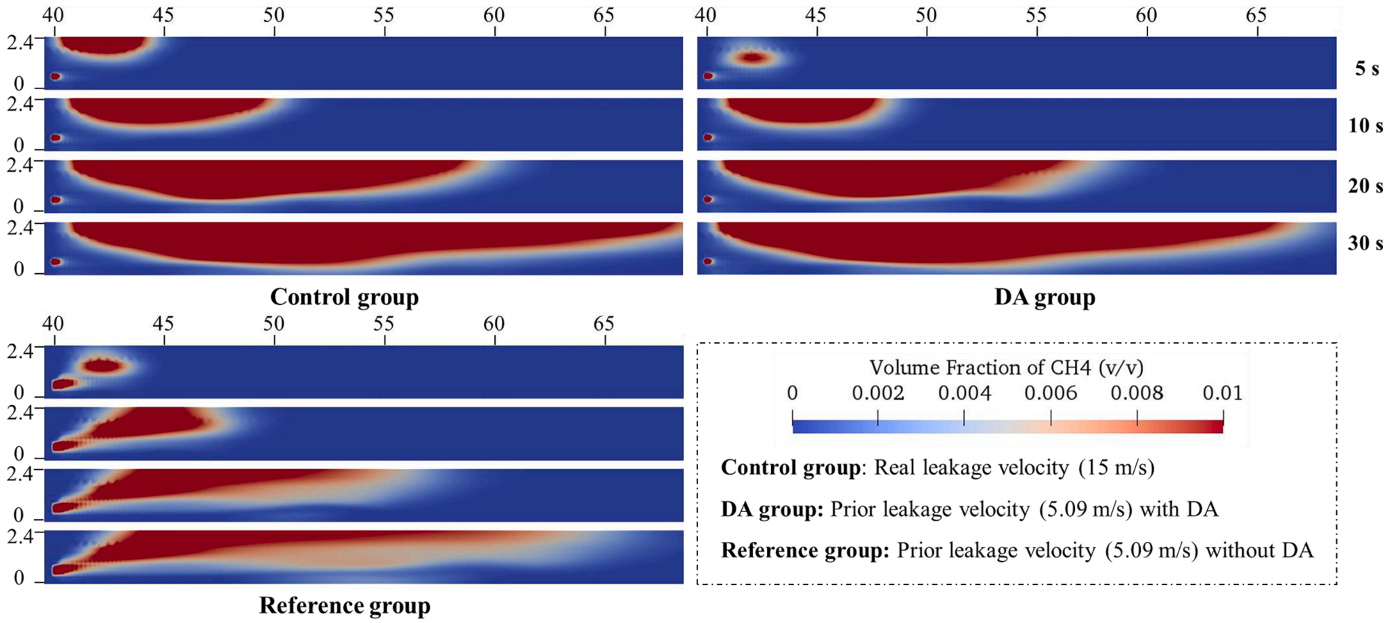

Fig. 8. Comparison between the control group, the DA group, and the reference group at $Y = 1$ m cross-section.

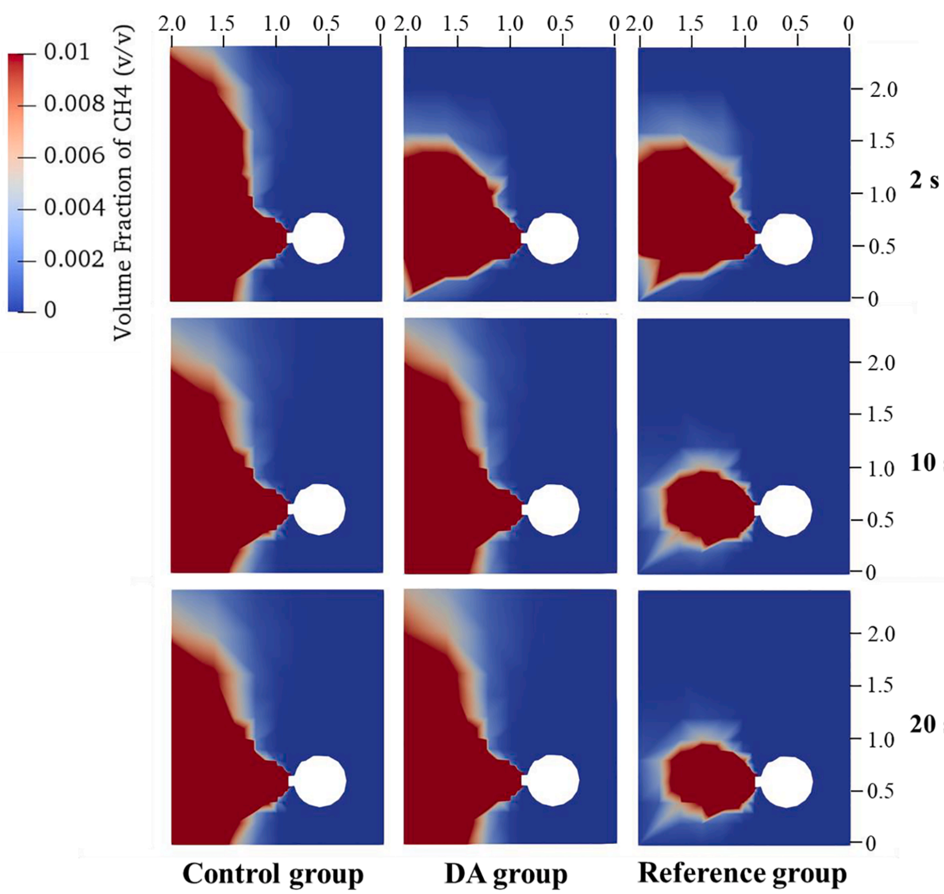

Fig. 9. Comparison between the control group, the DA group, and the reference group at $X = 40$ m cross-section.

stage ($T = 5$ s). There are two major reasons for this: (i) Although the prediction of the DA group is calculated by the mean of ensembles, there is a great similarity existing between the prior ensemble mean of the DA group and the leakage velocity of the reference group; (ii) At the initial stage of natural gas leakage, the DA algorithm can achieve negligible revision due to the limited observation data available. As time goes on, a phenomenon can be observed that the released gas was diluted rapidly in the reference group, which indicates a large deviation compared to the control group. This is because the reference group cannot be revised by the DA algorithm and the relatively low leakage velocity persist. Therefore, the gas concentration distribution shows a large difference between the reference group and the control group under the effect of dynamic ventilation. However, the gas concentration distribution of the DA group shows a comparable prediction compared to the control group. This is because the available observation data increased gradually, which were used to correct prior errors in the DA group and finally achieved a more accurate prediction of the gas concentration distribution. Similarly, the vertical concentration distribution of the DA group becomes more comparable to the real concentration distribution in the control group, which can be observed in Fig. 9. However, a difference still exists between the control group and the reference group because the prior errors in the leakage source term cannot be revised by data assimilation. Meanwhile, it can be seen that the data assimilation process in the horizontal and vertical sections is quite different in terms of time series. The reason for this may be that the vertical section is relatively small and narrow, in which the relatively steady condition can be achieved in a short time under the effect of dynamic ventilation. Overall, the 3D-STE model can realize the reasonable correction of the three-dimensional gas concentration distribution by assimilating observation data into the gas dispersion model.

According to the specific layout of observation sites in Fig. 7, the above-mentioned horizontal and vertical sections ($Y = 1$ m and $X = 40$ m) are distributed with 28 and 12 observation sensors, respectively. To evaluate the accuracy of the proposed model in handling the gas concentration correction where there is no observation sites distribution, the horizontal ($Y = 0.75$ m) and vertical sections ($X = 52.5$ m) are extracted for further comparison, which is shown in Figs. 10 and 11. It suggests that the gas concentration distribution of the DA group can obtain a good revision with the progress of data assimilation. Therefore, the proposed model can be helpful to realize the reasonable prediction of the gas concentration distribution in the whole computational domain even in the section without available observation data.

Furthermore, in order to evaluate the prediction accuracy of the proposed model quantitatively, four statistical performance measures (SPMs), i.e., the fractional bias (FB), the normalized mean square error (NMSE), the correlation coefficient (R), and the fraction of predictions within a factor of two of observations (FAC2) (Chang & Hanna, 2004), are employed for the quantitative comparison of specific gas concentration values at the observation sites. And the calculation of statistical performance measures, corresponding acceptable intervals, and ideal values are detailed in Table 4 (He, Liu, Li, Ma, Zhou & Zhou, 2021; Zhang, Su, Yuan, Chen & Huang, 2014). Where C_p and C_o are gas concentration values obtained from the model prediction and observation data, overbar ($\overline{C}$) represents the average over the dataset, σ is the standard deviation.

Fig. 12 presents the scatter plots of gas concentration extracted from the control group and DA group at observation sites, in which all 84 data points used for data assimilation are taken into account. There is a quite difference between observation data and the model prediction at 5 s, Almost all statistical performance measures show an unacceptable deviation compared with the corresponding ideal values except for a relatively reasonable value of FAC2. However, such a reasonable value is attributed to the poor performance of the FAC2 because little concentration information can be captured by observation sensors at the initial leakage stage, i.e., there are too many zero values in both observation data and model prediction. Therefore, the average value (0.8558) of the FAC2 cannot essentially reveal the model performance at $T = 5$ s. With the processing of data assimilation, the model predictions are well consistent with the observation data, in which all four statistical performance measures gradually approach the ideal values. In this study, a reasonable prediction can be achieved at $T = 20$ s and very optimistic results at $T = 30$ s, which means the errors resulting from initial-guess leakage velocity, dynamic ventilation, and complex facilities, can be successfully suppressed by the proposed model. Therefore, the proposed model has a significant effect on the improvement of gas leakage and dispersion prediction.

3.2.3. Estimation of gas leakage rate

Fig. 13 presents the revision process of the gas leakage rate by using the proposed model and the quantitative comparison between the real leakage rate and model prediction. It can be seen that there is an apparent underestimation existing in the leakage rate with 42.67% relative errors at the initial stage of the accidental leakage. That is because the initial-guess leakage velocity can only obtain limited revision due to the lack of observation data. As a growing amount of observation data are integrated into the gas dispersion CFD model, the reconstructed leakage velocity shows a gradual trend of approaching the real value. Finally, the estimation of leakage velocity became stable at around 17 m/s after 25 s, in which the convergence results of the 3D-STE model prediction have been achieved. The max relative error between the model prediction and the true value was 42.39% at the initial stage, and the relative error of the model prediction approach around 13.33% from 25 s to the end due to the estimation of leakage velocity became stable gradually. Therefore, it can be concluded that the proposed 3D-

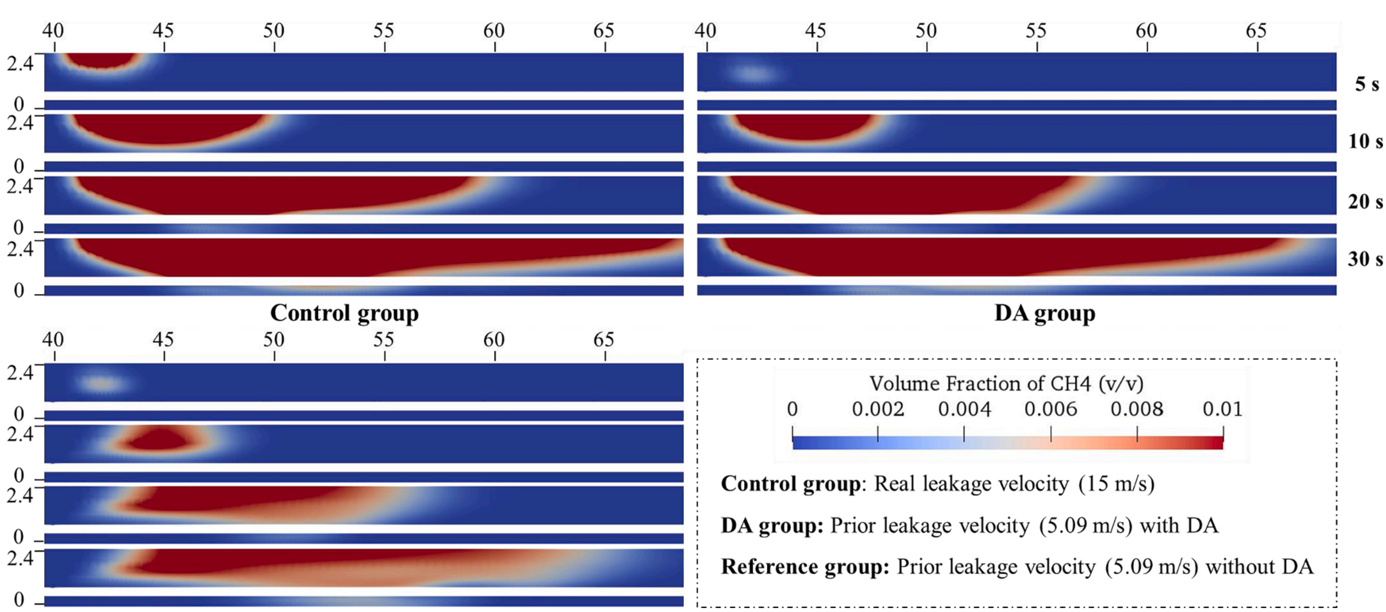

Fig. 10. Comparison between the control group, the DA group, and the reference group at $Y = 0.75$ m cross-section.

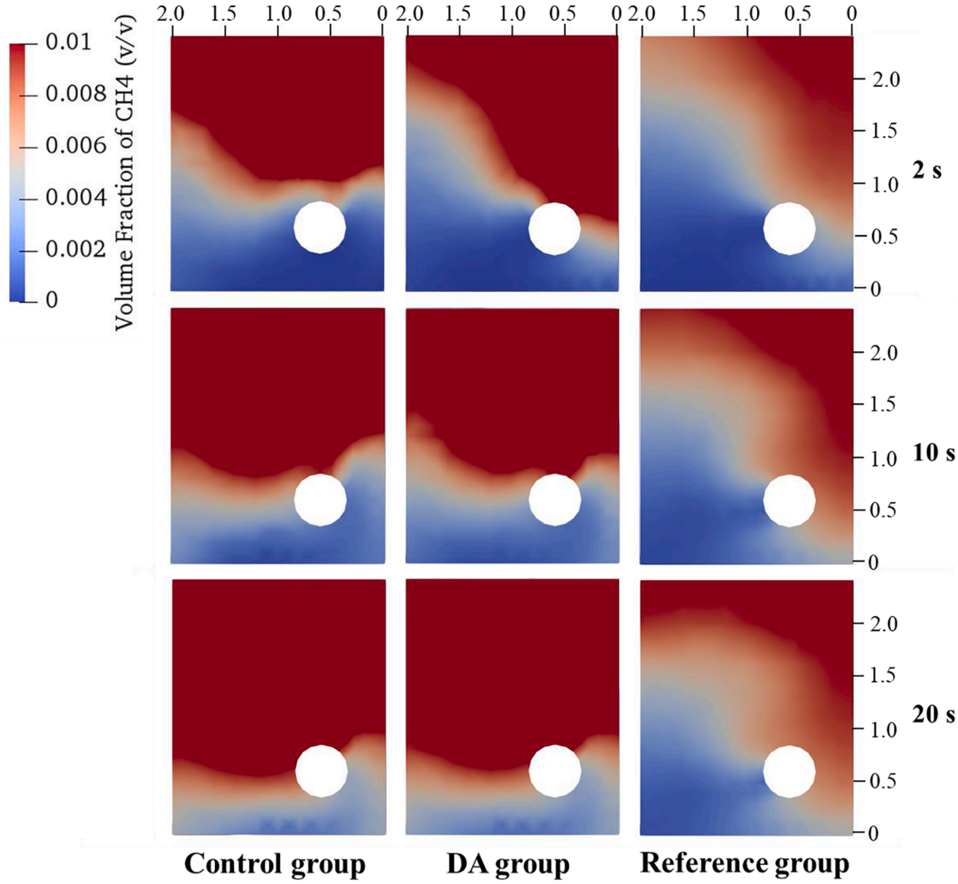

Fig. 11. Comparison between the control group, the DA group, and the reference group at $X = 52.5$ m cross-section.

Table 4
Calculation of statistical performance measures and corresponding acceptable intervals.

Name	Formula	Acceptable intervals	Ideal value
FB	$\frac{(\overline{C_o} - \overline{C_p})}{0.5(\overline{C_o} + \overline{C_p})}$	$-0.3 \leq FB \leq 0.3$	0
NMSE	$\frac{\overline{((C_o - C_p)^2)}}{\overline{C_o}\,\overline{C_p}}$	$NMSE \leq 4$	0
R	$\frac{\overline{((C_o - \overline{C_o})(C_p - \overline{C_p}))}}{\sigma_{C_p}\sigma_{C_o}}$	/	1
FAC2	$\frac{C_p}{C_o}$	$0.5 \leq FAC2 \leq 2$	1

STE model is an effective tool to provide a reasonable estimation of gas leakage velocity with high similarity to the actual leakage velocity despite huge errors existing in the initial-guess leakage velocity.

4. Application discussion

In this section, we present an exploratory discussion with an emphasis on the practical application of the proposed model in actual utility tunnels. A feasible framework is proposed to guide the application of this model for predicting gas leakage and dispersion and supporting emergency response treatment. Meanwhile, recommendations for future works are elaborated for improving the proposed model and facilitating the application of the proposed model.

4.1. A framework for 3D-STE model application

Compared to the previous studies on the source term estimation of gas leakage accidents in confined space scenarios, the proposed 3D-STE model integrated advantages of the three-dimensional CFD-based model and gas sensor networks while the EnKF algorithm helps to bridge the gap between simulation results and measurement data. Moreover, the dynamic ventilation pattern of utility tunnels is also involved. In summary, it obtains a good improvement in the following aspects:

(i) Except for reconstructing the leakage source, the three-dimensional spatiotemporal gas concentration distribution can be obtained by the proposed model because the CFD-based gas dispersion model is integrated accounting for three-dimensional facilities layout, turbulent diffusion, and gravity-driven multi-component transportation. Such a precise gas concentration distribution can provide more risk-related information for decision-makers such as dispersion distance and explosive area of leaking gas.

(ii) The dynamic ventilation pattern based on real-time alarm concentration allows a more realistic reproduction of the “two-stage” gas dispersion process dominated by normal and accidental ventilation conditions, respectively. It can help to reduce the difference between simulation results and actual situations, which benefits a more accurate consequence assessment.

Fig. 14 provides a feasible framework for the application of the 3D-STE model in actual utility tunnel scenarios. Firstly, the numerical model should be built according to the geometric characteristics of specific utility tunnels. In normal scenarios, i.e., no leakage occurrence, the available data collected by various sensors can be used to initialize the numerical model for simulating a steady flow field in advance. When an unexpected leakage accident happened, some theoretical and empirical methods can be employed to calculate the prior source term as

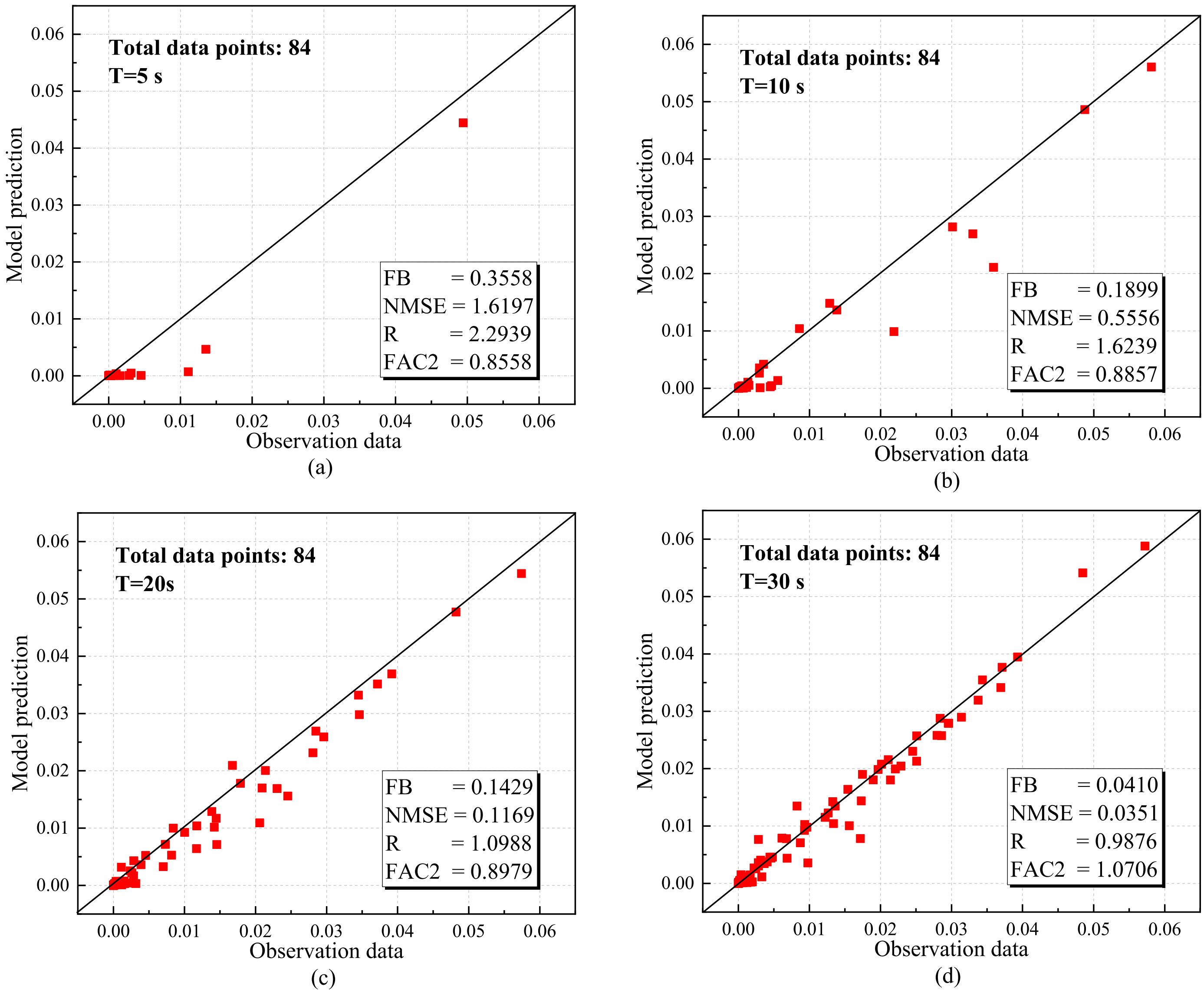

Fig. 12. Scatter plots of observation data and model prediction.

possible as close to the real source term. Then the 3D-STE model can predict the three-dimensional gas concentration distribution and reconstruct the source term by integrating the measurement data into numerical simulations. The real-time display of the prediction results can be obtained as well as some risk-related information such as source term, dispersion distance, and explosive area can be collected to support decision-making. Finally, the proposed 3D-STE model can be integrated into the digital system of utility tunnels. A smart platform and a data warehouse can be developed for the whole process management and data exploits of the digital system. Hence, it helps to assist safety operations of utility tunnels by furnishing control recommendations to decision-makers in accidental situations, such as manual shutdown, rush repair, and dynamic ventilation strategy.

4.2. Recommendation for future works

(1) Timely emergency response and risk treatment are urgent needs for accidental scenarios. Graphics Processor Units (GPUs) emerged as a major paradigm for resolving complicated computational tasks, making them more appealing for the solution of massive systems. Because both the algebraic matrix solving of the CFD model and the multi-ensemble structure of the EnKF model show good parallelism, the proposed 3D-STE model would achieve faster source term estimation and gas concentration distribution prediction by combining GPU speed-up techniques.

(2) The emerging data-driven techniques have great potential to be served as the surrogate model for either the CFD-based gas dispersion prediction model or the source term estimation model. Given the high data volume requirements of data-driven techniques, the developed gas dispersion model can be used to expand the data volume and help develop a more efficient gas dispersion prediction model. As more and more high-confidence data (e.g., experimental data and field test data) are available, the accurate source term estimation model is possible to be developed by using data-driven techniques.

(3) Moreover, the combination of the risk-based model can benefit the decision-making more comprehensively. With the combination of quantitative gas concentration distribution provided by the proposed model, the risk-based model can consider more risk-related factors such as ignition probability and safety barriers, which provide more comprehensive recommendations to the emergency response and risk treatment.

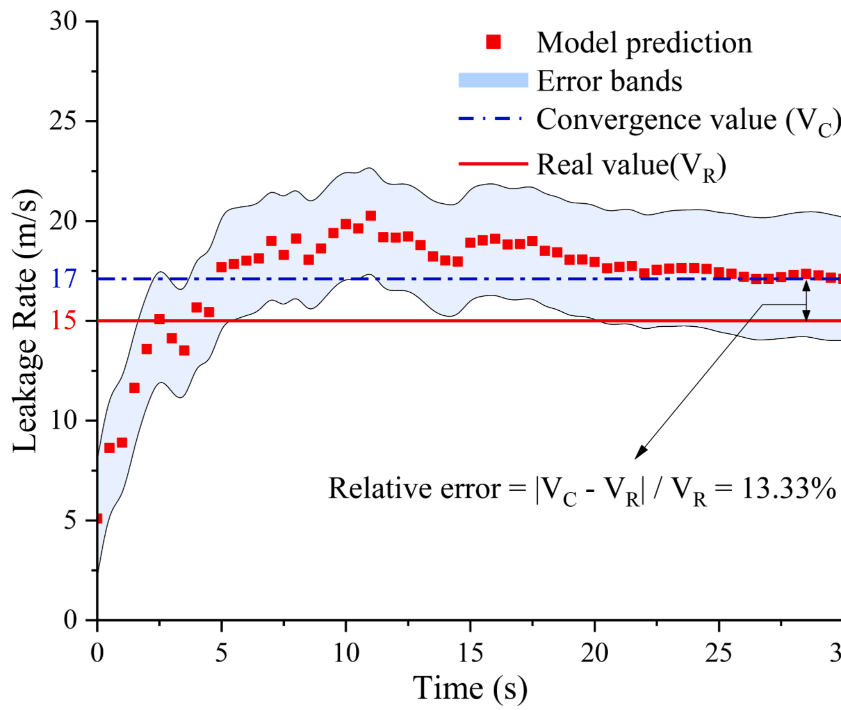

Fig. 13. Revision process of the leakage rate by the 3D-STE model.

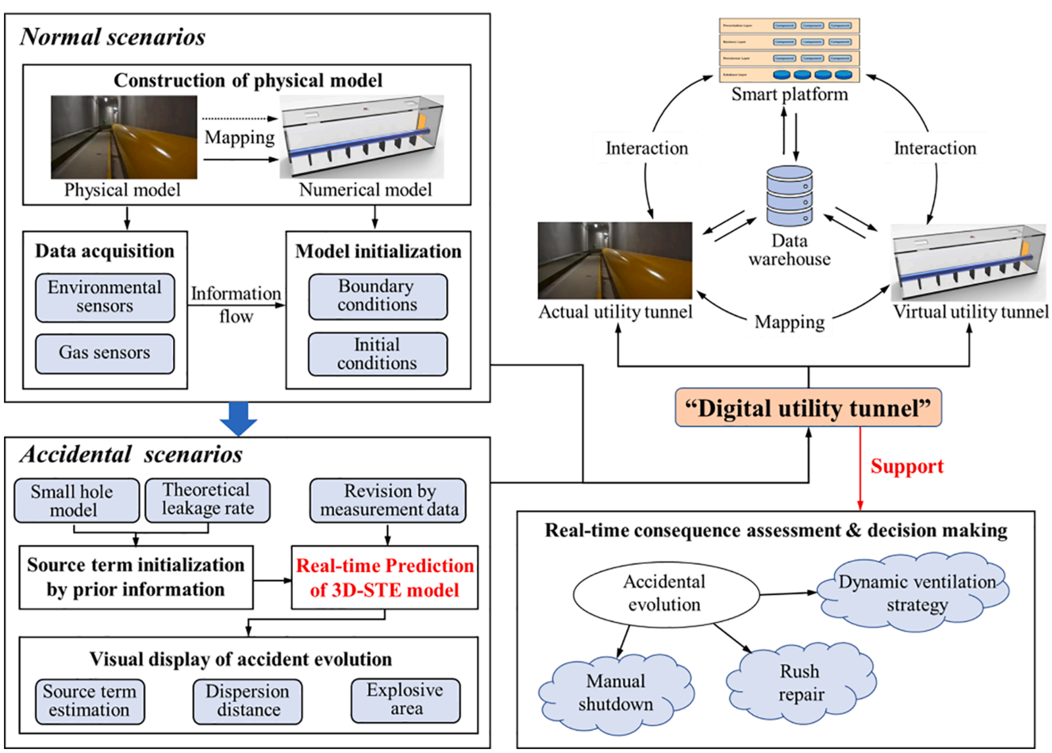

Fig. 14. Framework of the digital utility tunnel.

5. Conclusion

This study proposed a three-dimensional source term estimation (3D-STE) model with the integration of the CFD-based gas dispersion model and ensemble Kalman filter (EnKF) algorithm. It could be helpful to achieve improved three-dimensional gas concentration spatiotemporal distribution prediction and leakage source estimation based on available observation data.

The CFD-based gas dispersion model was developed based on the *rhoReactingBuoyantFoam* embedded in the OpenFOAM platform. And it was validated by experimental data obtained from a gas release scenario of the confined utility tunnel system. The results demonstrated that the simulation results calculated by the gas dispersion model are in good agreement with the experimental data. Therefore, this model can be utilized as an effective tool to simulate the natural gas leakage and dispersion characteristics in tunnel-related scenarios. The 3D-STE model is built based on the validated gas dispersion model and EnKF algorithm. And the twin experiment was designed to validate the effectiveness of the proposed model qualitatively and quantitatively. The results showed that this proposed model is capable of addressing the practical leakage accidents of the utility tunnel in the presence of dynamic ventilation conditions. The revised gas concentration spatiotemporal distribution and reasonable leakage source information can be obtained after a period of data assimilation, which aids in timely emergency response in the event of an unexpected leakage accident. Finally, a practical framework is elaborated and thus can provide guidance for the application of the 3D-STE model.

Declaration of Competing Interest

The authors declare that they have no known competing financial interests or personal relationships that could have appeared to influence the work reported in this paper.

Acknowledgments

This work was supported by the National Natural Science Foundation of China (Grant No. 52174223) and the National Key Research and Development Program of China (Grant No. 2017YFC0805001).

References

Anderson, J. (2007). An adaptive covariance inflation error correction algorithm for ensemble filters. *Tellus, 59*, 210–224.
Bai, Y., Zhou, R., & Wu, J. (2020). Hazard identification and analysis of urban utility tunnels in China. *Tunnelling and Underground Space Technology, 106*, Article 103584.
Broere, W. (2016). Urban underground space: Solving the problems of today's cities. *Tunnelling and Underground Space Technology, 55*, 245–248.
Bu, F., Liu, Y., Wang, Z., Xu, Z., Chen, S., & Hao, G. (2021). Analysis of natural gas leakage diffusion characteristics and prediction of invasion distance in utility tunnels. *Journal of Natural Gas Science and Engineering, 96*, Article 104270.
Cai, J., Wu, J., Yuan, S., Liu, Z., & Kong, D. (2021). Numerical analysis of multi-factors effects on the leakage and gas diffusion of gas drainage pipeline in underground coal mines. *Process Safety and Environmental Protection, 151*, 166–181.
Carneiro, F., Moura, L., Rocha, P., Lima, R., & Ismail, K. (2019). Application and analysis of the moving mesh algorithm AMI in a small scale HAWT: Validation with field test's results against the frozen rotor approach. *Energy, 171*, 819–829.
Chang, J., & Hanna, S. (2004). Air quality model performance evaluation. *Meteorology and atmospheric physics, 87*, 167–196.
Duan, R., Liu, W., Xu, L., Huang, Y., Shen, X., Lin, C. H., et al. (2015). Mesh type and number for the CFD simulations of air distribution in an aircraft cabin. *Numerical Heat Transfer, Part B: Fundamentals., 67*(6), 489–506.
Fang, Z., Lin, H., Huang, H., & Zheng, H. (2006). Experiment and numerical simulation of gas diffusion in utility tunnels. *Engineering mechanics, 23*(9), 189–192.
Fiates, J., Santos, R., Neto, F., Francesconi, A., Simoes, V., & Vianna, S. (2016). An alternative CFD tool for gas dispersion CFD modelling of heavy gas. *Journal of Loss Prevention in the Process Industries, 44*, 583–593.
He, J., Liu, L., Li, A., Ma, Y., Zhou, D., Zhou, Q., et al. (2021). A dense gas dispersion model based on revised meteorological parameters and its performance evaluation. *Atmospheric Environment, 344*, Article 117953.
Ji, J., Tong, Q., Wang, L., Lin, C., Zhang, C., Gao, Z., et al. (2018). Application of the EnKF method for real-time forecasting of smoke movement during tunnel fires. *Advances in Engineering Software, 115*, 398–412.
Katzfuss, M., Stroud, J., & Wikle, C. (2016). Understanding the ensemble Kalman filter. *The American Statistician, 70*, 350–357.
Kim, H., Park, M., Kim, C., & Shin, D. (2019). Source localization for hazardous material release in an outdoor chemical plant via a combination of LSTM-RNN and CFD simulation. *Computers and Chemical Engineering, 125*, 476–489.
Li, S., Liu, X., Wang, J., Zheng, Y., & Deng, S. (2019). Experimental reduced-scale study on the resistance characteristics of the ventilation system of a utility tunnel under different pipeline layouts. *Tunnelling and Underground Space Technology, 90*, 131–143.
Lin, C., & Wang, L. (2013). Forecasting simulations of indoor environment using data assimilation via an ensemble kalman filter. *Building and Environment, 64*(6), 169–176.
Liu, C., Wang, D., Guo, Y., Zhang, S., & He, R. (2019). Research on diffusion behaviors of leaked natural gas in urban underground utility tunnels. In *Proceedings of the 2019 IEEE International Conference on Mechatronics and Automation (ICMA).*. IEEE.
Lu, H., Huang, K., Fu, L., Zhang, Z., Wu, S., & Lyu, Y. (2018). Study on leakage and ventilation scheme of gas pipeline in tunnel. *Journal of Natural Gas Science and Engineering, 53*, 347–358.
Ma, D., Gao, J., Zhang, Z., & Zhao, H. (2021). Identifying atmospheric pollutant sources using a machine learning dispersion model and Markov chain Monte Carlo methods. *Stochastic Environmental Research and Risk Assessment, 311*, 237–245.
Ma, D., & Zhang, X. (2016). Contaminant dispersion prediction and source estimation with integrated Gaussian-machine learning network model for point source emission in atmosphere. *Journal of Hazardous Materials, 311*, 237–245.
Mack, A., & Spruijt, M. (2013). Validation of OpenFOAM for heavy gas dispersion applications. *Journal of Hazardous Materials, 262*, 504–516.
Marzouk, M., & Othman, A. (2020). Planning utility infrastructure requirements for smart cities using theintegration between BIM and GIS. *Sustainable Cities and Society, 57*, Article 102120.
Menter, F., Kuntz, M., & Langtry, R. (2003). Ten years of industrial experience with the SST turbulence model. In *Proceedings of the fourth international symposium on Turbulence. Heat and Mass Transfer* (pp. 625–632).
Ministry of Housing and Urban-Rural Development of the People's Republic of China. In . *GB 50838-2015 Technical code for urban utility tunnel engineering,* (2015)). Beijing: China Planning Press.
Sharma, H., Vaidya, U., & Ganapathysubramanian, B. (2019). Estimating contaminant distribution from finite sensor data: Perron Frobenious operator and ensemble Kalman Filtering. *Building and Environment, 159*, Article 106148.
Sklavounos, S., & Rigas, F. (2004). Validation of turbulence models in heavy gas dispersion over obstacles. *Journal of Hazardous Materials, 108*, 9–20.
Tan, C., Liu, Y., & Wang, T. (2017). CFD analysis of gas diffusion and ventilation protection in municipal pipe tunnel. In *Proceedings of the 2017 International Conference.*. ACM.
Wang, J., Zhao, J., Lei, X., & Wang, H. (2019). An effective method for point pollution source identification in rivers with performance-improved ensemble kalman filter. *Journal of Hydrology, 577*, Article 123991.
Wang, T., Tan, L., Xie, S., & Ma, B. (2018). Development and applications of common utility tunnels in China. *Tunnelling and Underground Space Technology, 76*, 92–106.
Wang, X., Tan, Y., Zhang, T., Zhang, J., & Yu, K. (2020). Diffusion process simulation and ventilation strategy for small-hole natural gas leakage in utility tunnels. *Tunnelling and Underground Space Technology, 97*, Article 103276.
Wang, Y., Huang, H., Huang, L., & Ristic, B. (2017). Evaluation of Bayesian source estimation methods with Prairie Grass observations and Gaussian plume model: A comparison of likelihood functions and distance measures. *Atmospheric Environment, 152*, 519–530.
Wu, J., Cai, J., Yuan, S., Zhang, X., & Reniers, G. (2021). CFD and EnKF coupling estimation of LNG leakage and dispersion. *Safety Science, 139*, Article 105263.
Wu, J., Liu, Z., Yuan, S., Cai, J., & Hu, X. (2020). Source term estimation of natural gas leakage in utility tunnel by combining CFD and Bayesian inference method. *Journal of Loss Prevention in the Process Industries, 68*, Article 104328.
Wu, J., Yuan, S., Zhang, C., & Zhang, X. (2018). Numerical estimation of gas release and dispersion in coal mine using ensemble Kalman filter. *Journal of Loss Prevention in the Process Industries, 56*, 57–67.
Xue, F., Kikumoto, H., Li, X., & Ooka, R. (2018). Bayesian source term estimation of atmospheric releases in urban areas using LES approach. *Journal of Hazardous Materials, 349*, 68–78.
Xue, F., Li, X., & Zhang, W. (2017). Bayesian identification of a single tracer source in an urban-like environment using a deterministic approach. *Atmospheric Environment, 164*, 128–138.
Yang, C., Peng, F., Xu, K., & Zheng, L. (2019). Feasibility study on the geothermal utility tunnel system. *Sustainable Cities and Society, 46*, Article 101445.
Yin, X., Liu, H., Chen, Y., Wang, Y., & AI-Hussein, M. (2020). A BIM-based framework for operation and maintenance of utility tunnels. *Tunnelling and Underground Space Technology, 97*, Article 103252.
Yuan, S., Wu, J., Zhang, X., & Liu, W. (2019). EnKF-based estimation of natural gas release and dispersion in an underground tunnel. *Journal of Loss Prevention in the Process Industries, 62*, Article 103931.
Zhang, P., & Lan, H. (2020). Effects of ventilation on leakage and diffusion law of gas pipeline in utility tunnel. *Tunnelling and Underground Space Technology, 105*, Article 103557.
Zhang, X., & Huang, M. (2017). Ensemble-based release estimation for accidental river pollution with known source position. *Journal of Hazardous Materials, 333*, 99–108.
Zhang, X., Li, Q., Su, G., & Yuan, M. (2015a). Ensemble-based simultaneous emission estimates and improved forecast of radioactive pollution from nuclear power plant accidents: Application to ETEX tracer experiment. *Journal of Environmental Radioactivity, 142*, 78–86.
Zhang, X., Su, G., Chen, J., Raskob, W., Yuan, H., & Huang, Q. (2015b). Iterative ensemble Kalman filter for atmospheric dispersion in nuclear accidents: An application to Kincaid tracer experiment. *Journal of Hazardous Materials, 297*, 329–339.
Zhang, X., Su, G., Yuan, H., Chen, J., & Huang, Q. (2014). Modified ensemble Kalman filter for nuclear accident atmospheric dispersion: Prediction improved and source estimated. *Journal of Hazardous Materials, 280*, 143–155.
Zhou, K., Li, F., Cai, H., Jing, Y., Zhuang, J., Li, M., et al. (2022). Estimation of the natural gas leakage source with different monitoring sensor networks in an underground utility Tunnel: From the perspectives of energy security. *Energy and Building, 254*, Article 111645.
Zhou, K., Li, F., Cai, H., Yang, Y., Peng, F., Chen, L., et al. (2021). Experimental and numerical investigation of gas diffusion under an urban underground construction. *Energy and Built Environment, 2*, 436–444.